Force measurement reveals structure of a confined liquid: Observation of the impenetrable space

Ken-ichi Amano[1], Eisuke Tanaka[1], Kazuya Kobayashi[1], Hiroshi Onishi[2], Naoya Nishi[1], and Tetsuo Sakka[1]

[1]*Department of Energy and Hydrocarbon Chemistry, Graduate School of Engineering, Kyoto University, Kyoto* 615-8510, *Japan.*

[2]*Department of Chemistry, School of Science, Kobe University, Nada-ku, Kobe* 657-8501, *Japan.*

Corresponding author: Ken-ichi Amano.

Electric mail: amano.kenichi.8s@kyoto-u.ac.jp

ABSTRACT
Understanding of structure of a confined liquid is an important subject for developments of surface science, tribology, biophysics, etc. In this study, we propose its measurement theory and conduct a test of the theory. The measurement theory uses a force curve obtained by surface force apparatus, and transforms the force curve into the confined liquid structure. To check validity of the measurement theory, we perform a verification test in a computer. It is found that the theory can semi-quantitatively reproduce the confined liquid structure. The theory will lead to the first step towards measuring a liquid structure confined between optically impenetrable substrates.

1. Introduction

Recently, structural analyses of nano-materials and nano-systems are important subjects. Similarly, the analysis of a confined liquid structure is also important, because it is related to surface science, tribology, biophysics, and so on. The confined liquid structure has been experimentally studied by several researchers using, e.g., surface force apparatus (SFA) and atomic force microscopy (AFM). The studies by SFA [1-6] have revealed the peculiar phenomena of the confined liquid: Oscillatory force between the two surfaces, symptoms of evaporation and solidification, rapid increase of the liquid's viscosity. AFM has also revealed the confined liquid's property [7-9]. Although these instruments can detect the oscillatory force suggesting structural layering within the confined space between the probe and the sample surface, they have not directly measured the structure of the confined liquid itself. On the other hand, x-ray and neutron experiments are able to measure the confined liquid structure [10-12] as well as the structures of liquid/air [13,14], liquid/liquid [15], liquid/solid [16-18] interfaces by analyzing these experimental results. The x-ray and neutron experiments are useful for determination of the confined liquid structures, however, many of the structures have not been measured due to its difficulties of the experimental setup and condition. The confined liquid structure has been studied also by statistical mechanics of liquids [19-21], density functional theory [22,23], and simulations [24-28]. These theoretical studies have indicated the structural layering within the confined space and the local phase transitions. In this way, the confined liquid structures have been experimentally and theoretically studied much, and these studies are significant for elucidation of the properties of the confined liquids.

In this study, we present a measurement theory (a theory for the experiment) which calculates the confined liquid structure from the force curve obtained by SFA. Here, we call it the transform theory. The transform theory has two advantages. One is that one can obtain the liquid structure without x-ray and neutron. The other is that one can obtain the liquid structure even if the substrates are opaque, because recent SFA named twin-path SFA [6] can use opaque substrates in the measurement of the force curve. Of course, the both SFA and transform theory have weak points in accuracies at the present time. However, in our view, this measurement strategy is important to obtain the confined liquid structure between the opaque substrates. The transform theory plays an important role when the force curve is interpreted as or compared with the liquid structure.

Transformation from the force curve into the solvation structure (local liquid structure) is comparatively a new subject. In 2010, Kimura *et al.* [29] have derived a simple relationship between the force curve measured by AFM and the liquid structure on a single surface (not confined). In the theory, the tip apex is approximated by a delta

function and there are no consideration about volume of the probe and solvent's entropy. According to the theory, the AFM probe receives zero force when it overlaps with the solid surface. (When the probe *overlaps* with the solid surface, it should receive strong repulsive force.) Then, recently Watkins *et al.* [30] and Amano *et al.* [31] independently proposed a relational expression by approximating the probe as one solvent molecule (it is called the ideal probe). It has been found that the theory functions when the solvent molecule or a very similar one is located on the tip apex. Therefore, it has been concluded that a nearly-ideal probe is required in the real experiment in order to precisely measure the solvation structure [31]. Just recently, the transform theory for SFA has also been proposed by Amano and Takahashi [32]. In the theory, the solvent molecule is approximated by a sphere and two-body potential between solvent molecules is arbitrary. However, two-body potential between the solvent molecule and solid surface (SFA probe) is approximated to rigid. Using the theory, the liquid structure on the single surface was reproduced from the force curve. It has been found that the force is proportional to the liquid density on the contact surface and the theory works better when the number density of the solvent is lower and the two-body potential between solvent molecule and solid plate is close to the rigid potential.

The outline of the paper is as follows. The theoretical and computational details of the transform theory are given in Chapters 2.1 and 2.2, respectively. To check validity of the transform theory, its verification test is performed in a computer, results of which are shown in Chapter 3. In the test, a force curve between two walls is numerically calculated by using a traditional liquid theory. Then, the force curve is substituted into the transform theory as an input. This computational test is important for practical realization of the theory. It will be shown that the transform theory can semi-quantitatively reproduce the confined liquid structure. Finally, in Chapter 4, the conclusions are written.

2. Theory and computation

2.1. *Theoretical details*

To calculate the confined liquid structure from the force curve, two transform theories are used. One is an application of the theory written in [32]. In the theory, the two solid surfaces are rigid wall, and thus we call it RW theory. On the other transform theory, the two solid surfaces have soft potential with rigid wall with the solvent molecule, i.e., two-body potential between the solid surface and the solvent molecule is soft potential with rigid wall [33]. Therefore, we call it SPRW theory. *Two key*

concepts for calculation of the confined liquid structure are (I) there is information about the confined liquid structure in the force curve, i.e., the force curve is determined by the confined liquid structure; (II) the information about the confined liquid structures are *preserved* in the liquid structure on a single wall calculated by RW and SPRW theories, because Kirkwood superposition approximation [34-36],

$$\rho(z; s) = \rho_0 g_{\text{tot}}(z; s) \approx \rho_0 g_1(z) g_2(z - s), \tag{1}$$

used in RW and SPRW theories cannot offset the compression phenomenon of the interlayer spacing caused by the sandwiching, i.e., the liquid structures on a single wall calculated by RW and SPRW theories essentially include properties of the confined liquid structures. Here, ρ is the number density of the confined liquid, ρ_0 is the bulk number density (which is constant), g_{tot} is the normalized number density of the confined liquid, and g_i (i = 1 or 2) is a pair correlation function between the solid i and solvent (g_i is the so-called a normalized number density of the solvent or a solvation structure). We notify that g_i is that for an isolated solid i. In other words, the solid i immersed in the bulk solvent has the solvation structure g_i on its flat surface. z and s represent displacement from the center of circular surface of the solid 1 and separation between solid plates 1 and 2 (see Fig. 1). The key concepts above lead to that the confined liquid structure can be calculated by following procedure: (A) calculate the liquid structure on a single wall by using RW or SPRW theory; (B) calculate the confined liquid structure by reusing Kirkwood superposition approximation. (The confined liquid structure can be reproduced by mixing g_1 and g_2, because they, calculated by RW or SPRW theory, essentially contain information about confined liquid structure.)

The derivation process of the SPRW theory [33] is explained here. In our earlier work [32], the transformation is performed by modeling the two-body potential between the solid surface and the solvent molecule as the rigid potential. However, the approximation was very rough. It should be improved to a more realistic model. Hence, the two-body potential for SPRW theory is modeled as attractive (or repulsive) soft potential with rigid wall. SPRW theory is derived based on the statistical mechanics of simple liquids. The theoretical conditions are as follows: The two same solids with flat surfaces are immersed in the solvent; Their flat surfaces are parallel; The thickness of the solid is sufficiently long; The diameter of the solvent molecule is d_S (arbitrary value); Two-body potential between the solvent molecules is arbitrary shape, whereas two-body potential between the solid plate and the solvent molecule is attractive (or repulsive) soft potential with rigid wall. In SFA experiment, the force between two surfaces is measured, and the solvation force can be extracted from the crude force (total force) by subtracting two-body force between the solid plates. That is, $f_{\text{sol}} = f_{\text{all}} - f_2$, where f_{sol}, f_{all}, and f_2 represent the solvation force, total force, and two-body force,

respectively. The two-body force can be measured in the air (vacuum) or theoretically calculated. The solvation force along the z-axis (which acts on the cylindrical solid 2) has a relationship with the number density distribution of the liquid. It can be expressed as [24,32]

$$f_{sol}(s) = A \int_{-\infty}^{\infty} \rho(z; s) \frac{\partial u_2(z; s)}{\partial z} dz, \tag{2}$$

where A represents surface area of the flat surface i.e., circular surface area of the cylindrical solid 2 (see Fig. 1). $\rho(z;s)$ is the number density of the solvent at z, where the separation between the cylindrical solids is s. u_2 is the two-body potential between cylindrical solid 2 and the solvent molecule. Here, Kirkwood superposition approximation [24,32-36] is applied to ρ, and then Eq. (2) becomes

$$f_{sol}(s) = A\rho_0 \int_0^s g_1(z)g_2(z-s)u_2'(z-s)dz - PA, \tag{3}$$

where u_2' represents the partial differentiation of u_2 with respect to z, and P represents the solvent's pressure on a wall. $-PA$ represents the solvation force acting on the upside of the solid 2, the value of which is always constant because the solvation structure on it does not change. The partial differentiation of u_2 with respect to z (u_2') can be expressed as

$$u_2'(z-s) = -k_B T \exp[u_2(z-s)/(k_B T)] \frac{\partial \exp[-u_2(z-s)/(k_B T)]}{\partial z}, \tag{4}$$

where k_B and T are the Boltzmann constant and absolute temperature, respectively. Consequently, the partial differentiation at the contact point (downside) is expressed as

$$u_2'(z-s)|_{DC} = k_B T \delta[z - (s - d_S/2)], \tag{5}$$

where δ is the delta function and the subscript DC means the downside-contact point. By substituting Eq. (5) into Eq.(3), $f_{sol}(d_S)$ is calculated to be

$$f_{sol}(d_S) = A k_B T \rho_0 g_1(d_S/2)g_2(-d_S/2) - PA, \tag{6}$$

where the values of $g_1(d_S/2)$ and $g_2(-d_S/2)$ both are the normalized number density at the contact points. They are represented as g_C where the subscript C denotes the contact point. Therefore, g_C is given by

$$g_C = \sqrt{\frac{f_{sol}(d_S) + PA}{Ak_BT\rho_0}}. \tag{7}$$

Secondly, we consider $f_{sol}(d_S+\Delta s)$ to obtain $g_1(d_S/2+\Delta s)$, where Δs is the sufficiently small separation. $f_{sol}(d_S+\Delta s)$ is expressed as

$$\begin{aligned}f_{sol}(d_S + \Delta s) = {}& A\rho_0 g_1(d_S/2)g_2(-d_S/2 - \Delta s)u_2'(-d_S/2 - \Delta s)\Delta s \\ &+ Ak_BT\rho_0 g_1(d_S/2 + \Delta s)g_2(-d_S/2) - PA.\end{aligned} \tag{8}$$

In the theoretical condition, the solids 1 and 2 are the same things. Thus, Eq. (8) is rewritten as

$$\begin{aligned}f_{sol}(d_S + \Delta s) = {}& A\rho_0 g_C g_1(d_S/2 + \Delta s)u_2'(-d_S/2 - \Delta s)\Delta s \\ &+ Ak_BT\rho_0 g_1(d_S/2 + \Delta s)g_C - PA.\end{aligned} \tag{9}$$

Hence, $g_1(d_S/2+\Delta s)$ is given by

$$g_1(d_S/2 + \Delta s) = \frac{f_{sol}(d_S + \Delta s) + PA}{A\rho_0 g_C[k_BT + u_2'(-d_S/2 - \Delta s)\Delta s]} \tag{10}$$

Thirdly, we consider $f_{sol}(d_S+n\Delta s)$ to obtain $g_1(d_S/2+n\Delta s)$, where n represents arbitrary natural number. $f_{sol}(d_S+n\Delta s)$ is expressed as

$$\begin{aligned}f_{sol}(d_S + n\Delta s) = {}& A\rho_0 g_C g_2(-d_S/2 - n\Delta s)u_2'(-d_S/2 - n\Delta s)\Delta s \\ &+ A\rho_0 \sum_{i=1}^{n-1} g_1(d_S/2 + i\Delta s)g_2(-d_S/2 - (n-i)\Delta s)u_2'(-d_S/2 - (n-i)\Delta s)\Delta s \\ &+ Ak_BT\rho_0 g_1(d_S/2 + n\Delta s)g_C - PA.\end{aligned} \tag{11}$$

Therefore, $g_1(d_S/2+n\Delta s)$ is given by

$$g_1(d_S/2 + n\Delta s) = \frac{f_{sol}(d_S + n\Delta s) + PA - A\rho_0 \sum_{i=1}^{n-1} W(i)}{A\rho_0 g_C[k_BT + u_2'(-d_S/2 - n\Delta s)\Delta s]}, \tag{12}$$

where

$$W(i) = g_1(d_S/2 + i\Delta s)g_2(-d_S/2 - (n-i)\Delta s)u_2'(-d_S/2 - (n-i)\Delta s)\Delta s. \tag{13}$$

In the calculation of SPRW theory, separation between the flat surfaces s is stepwisely

6

increased, and the values of g_C, $f_{sol}(d_S+\Delta s)$, $f_{sol}(d_S+2\Delta s)$, $f_{sol}(d_S+3\Delta s)$, $\cdots$, $f_{sol}(d_S+n\Delta s)$ are obtained in turn, i.e., the values are sequentially calculated. Finally, the confined liquid structure ($g_{tot}(z;s)$) is calculated by substituting the results of g_1 and g_2 into Eq. (1). Since the Kirkwood superposition approximation is recycled, the compressed-interlayer spacing preserved in g_i is reflected in $g_{tot}(z;s)$. That is, the compressed liquid structure is restored.

When u_2 is not soft potential with rigid wall, but purely rigid one, SPRW theory must be the same as RW theory. Substituting the rigid potential into u_2 and $PA = Ak_BT\rho_0g_C$ [32], we have confirmed that the SPRW theory exactly coincides with RW theory,

$$g_1(s - d_S/2) = \frac{f_{sol}(s)}{Ak_BT\rho_0g_c} + 1, \tag{14}$$

where

$$g_C = \frac{1 + \sqrt{1 + 4f_{sol}(d_S)/(Ak_BT\rho_0)}}{2}. \tag{15}$$

To check the transform accuracy of the confined liquid structure, we compare the structures calculated by (i) a basic integral equation theory (three-dimensional Ornstein-Zernike equation coupled with a hypernetted-chain closure: 3D-OZ-HNC) [19-21,37], (ii) RW theory [32], and (iii) SPRW theory [33]. The confined liquid structures calculated by RW and SPRW theories are obtained through the process: (a) calculate the solvation structure around a pair of the cylindrical solids with the separation s by using 3D-OZ-HNC; (b) calculate the solvation force acting on the cylindrical solid 2 by using Eq. (2) of 3D version; (c) transform the solvation force into the solvation structure (g_1) on the flat surface of the isolated cylindrical solid 1 by using RW or SPRW theory; (d) since the cylindrical solids 1 and 2 are the same, g_2 is readily obtained from g_1; (e) the confined liquid structure is calculated by substituting g_1 and g_2 into Eq. (1). Here, the confined liquid structure calculated solely by 3D-OZ-HNC is the benchmark structure. If the shape of the confined liquid structure calculated by the transform theory is very similar to the benchmark structure, it means that the transformation from the solvation force is well-functioning.

2.2. *Computational details*

Models of the solvent molecule and the cylindrical solid for check of the

transform accuracy are as follows. Two-body potential between the solvent molecules being u_{SS} is following

$$u_{SS}(r) = \infty \qquad\qquad \text{for} \quad r < d_S, \tag{16a}$$
$$u_{SS}(r) = -\varepsilon(d_S/r)^6 \qquad \text{for} \quad r \geq d_S, \tag{16b}$$

where attractive parameter between the solvent molecules being ε is set at $1.0k_BT$ [32,38], and r represents the distance between the centers of the solvent molecules. Two-body potential between the cylindrical solid and the solvent molecule being u_{DS} (i.e., u_2) is written as

$$u_{DS}(h) = \infty \qquad\qquad\qquad\qquad \text{for} \quad h < d_S/2, \tag{17a}$$
$$u_{DS}(h) = -(\xi/8)(d_S/h)^3 \exp[-(h/10d_S)^{10}] \quad \text{for} \quad h \geq d_S/2, \tag{17b}$$

where the attractive parameter between the cylindrical solid and solvent molecule being ξ is set at $1.0k_BT$ [24-28,31,32,39], h represents the distance between the nearest surface of the cylindrical solid and the center of the solvent molecule, and $\exp[-(h/10d_S)^{10}]$ is cut off. These potentials are substituted into (1D and) 3D-OZ-HNC [19-21,37], and then the confined solvation structure followed by the solvation force are calculated. The confined solvation structure corresponds to a benchmark structure for the verification test and the solvation force is the input for the transform theory.

It is notified before the computational test that the width of Δs must be sufficiently small. Seeing Eq. (12), one can realize that its denominator must be an positive value, because $g_1(d_S/2+n\Delta s)$ and its numerator are positive values. That is, the following relation must be realized:

$$k_BT + u_2'(-d_S/2 - n\Delta s)\Delta s > 0. \tag{18}$$

Hence, the value of Δs must be within

$$0 < \Delta s < -k_BT/u_2'(-d_S/2 - n\Delta s). \tag{19}$$

In the case of the computational test, slope of the attractive soft potential u_2 becomes steeper as the position approaches the rigid wall. Therefore, the numerical range is rewritten as

$$0 < \Delta s < -k_BT/u_2'(-d_S/2 - \Delta s). \tag{20}$$

In the computational test (theoretical verification) of the transform theory, f_{sol} is obtained by using both 3D-OZ-HNC and Eq. (2) of 3D version. In other words, f_{sol} is

obtained by substituting the original confined liquid structure g_{bm} (which is calculated by 3D-OZ-HNC) into Eq. (2) of 3D version. The subscript "bm" represents "benchmark". This f_{sol} is substituted into RW or SPRW theory to obtain g_1. Then, g_2 is readily obtained from g_1, because the cylindrical solids 1 and 2 are the same. Finally, g_{tot} is calculated by using Eq. (1): $g_{\text{tot}}(z;s) \approx g_1(z)g_2(z - s)$. Here, we express the g_{tot} calculated through this process as g_{x}. If the shape of g_{x} is very similar to that of g_{bm}, it can be said that the theory we proposed here is valid.

3. Results and discussion

In what follows, the comparison among the results calculated by 3D-OZ-HNC (benchmark), RW theory, and SPRW theory is done with several separations ($s = 1.5d_{\text{S}}$, $2.0d_{\text{S}}$, $2.5d_{\text{S}}$, $3.0d_{\text{S}}$, $3.5d_{\text{S}}$, $4.0d_{\text{S}}$, $4.5d_{\text{S}}$, and $5.0d_{\text{S}}$). Figure 2 shows the confined liquid structures, where blue solid, green dashed, red dotted curves represent that calculated by 3D-OZ-HNC (benchmark), RW theory, and SPRW theory, respectively. The confined liquid structures take oscillatory shapes. The interlayer spacings are about d_{S} and the contact value is relatively high. Generally, it seems that reproducibility of the liquid structure is higher when s is the integral multiple of d_{S}.

As shown in Fig. 2, one can find that the deviation from the benchmark structure is not so large for RW and SPRW theories. However, the deviation tends to be large when $s = 1.5d_{\text{S}}$, $2.5d_{\text{S}}$, $3.5d_{\text{S}}$. Then, we calculated root mean square deviation (RMSD) of each curve by defining it as

$$\text{RMSD} \equiv \sqrt{\frac{1}{s}\int_0^s (g_{\text{x}}(z) - g(z)_{\text{bm}})^2 dz}, \tag{21}$$

where g_{x} and g_{bm} are the confined liquid structures that calculated by the transform theory (RW or SPRW theory) and by 3D-OZ-HNC (benchmark), respectively. As shown in Fig. 3, in most of the cases, RMSD values of SPRW theory are lower than those of RW theory. However, when $s = 1.5d_{\text{S}}$, RMSD value of SPRW theory is higher than that of RW theory.

The deviation from the benchmark structure is mainly caused by Kirkwood superposition approximation. Kirkwood superposition approximation can be written with potential of mean forces,

$$g_{\text{tot}} \approx \exp[-(\varphi_1 + \varphi_2)/(k_B T)], \tag{22}$$

where φ_i ($i = 1$ or 2) is potential of mean force between the cylindrical solid i and the solvent molecule. From Eq. (22), one can realize that this approximation is exact when the cylindrical solids 1 and 2 are sufficiently separated. Moreover, it is exact in which only three bodies, a solvent molecule and cylindrical solids 1 and 2, exist in the system. In the present case, however, the separation between the cylindrical solids 1 and 2 is very short, and there are so many solvent molecules around/between them. Therefore, the deviation is produced. In our opinion, improvement of Kirkwood superposition approximation or proposition of another approximation is the key to development of the transform theory. (We have confirmed that a linear superposition approximation cannot be the candidate for the improvement [24,32]; not shown here.)

4. Conclusions

In summary, we have proposed the transform theory for obtaining the confined liquid structure from the force curve. The detailed explanation of it has been presented in this paper. We have confirmed that the transform theory can reproduce the confined liquid structures when the system follows the theoretical condition to some extent. It has been found in the computed system that SPRW theory generally gives more precise results compared with RW theory. Using the theory, one can assess the confined liquid structure without x-ray and neutron, and hence optically impenetrable space can be observed by our theory. In the near future, we will apply the transform theory to a real SFA experiment. In addition, we will apply the theory to observation of the density distribution of colloids (micelles) [40,41]. Since the theory cannot be used for all of the experimental conditions due to the theoretical restriction, we should improve the theory to more practical level. For example, more universalistic two-body potential between the substrate and the small sphere should be introduced to the transform theory (elimination of the rigid wall). In the real SFA experiment, the substrate is not flat but cylindrical, the transform theory should take into account the shape of the cylinder. This new factor can be combined with the transform theory by utilizing Derjaguin approximation [42,43] or FPSE (force to pressure on a surface element) conversion [44,45]. The combined approach for cylindrical substrate will be explained in our future article. Measurements of the liquid structure on a single wall and the confined liquid structure are the important topics for structural analyses of nano-spaces. Development of the theories which transform the force curves measured by AFM and leaser tweezers into the liquid structures are also in our interests. We believe that the present theory becomes one of the basic theories for measurement of the liquid structure.

ACKNOWLEDGEMENTS

REFERENCES

[1] R. G. Horn and J. N. Israelachvili, J. Chem. Phys. 75 (1981) 1400.

[2] J. N. Israelachvili and P. M. McGuiggan, Science **241**, 795 (1988).

[3] H. K. Christenson, Chem. Phys. Lett. **118**, 455 (1985).

[4] J. Klein and E. Kumacheva, Science **269**, 816 (1995).

[5] U. Raviv, P. Laurat, J. Klein, Nature **413**, 51 (2001).

[6] H. Kawai, H. Sakuma, M. Mizukami, T. Abe, Y. Fukao, H. Tajima, and K. Kurihara, Rev. Sci. Instrum. **79**, 043701 (2008).

[7] T. Fukuma, Y. Ueda, S. Yoshioka, and S. Asakawa, Phys. Rev. Lett. **104**, 016101 (2010).

[8] T. Hiasa, K. Kimura, and H. Onishi, Phys. Chem. Chem. Phys. **14**, 8419 (2012).

[9] H. Imada, K. Kimura, and H. Onishi, Langmuir **29**, 10744 (2013).

[10] E. Perret, K. Nygård, D. K. Satapathy, T. E. Balmer, O. Bunk, M. Heuberger, and J. F. van der Veen, Europhys. Lett. **88**, 36004 (2009).

[11] E. Perret, K. Nygård, D. K. Satapathy, T. E. Balmer, O. Bunk, M. Heuberger, and J. F. van der Veen, J. Cynchrotron Rad. **17**, 465 (2010).

[12] J. Jelassi, T. Grosz, I. Bako, M.-C. Bellissent-Funel, J. C. Dore, H. L. Castricum, and R. Sridi-Dorbez, J. Chem. Phys. **134**, 064509 (2011).

[13] A. Braslau, M. Deutsch, P. S. Pershan, A. H. Weiss, J. Als-Nielsen, and J. Bohr, Phys. Rev. Lett. **54**, 114 (1985).

[14] N. Nishi, Y. Yasui, T. Uruga, H. Tanida, T. Yamada, S. Nakayama, H. Matsuoka, and T. Kakiuchi, J. Chem. Phys. 132, 164705 (2010).

[15] N. Laanait, M. Mihaylov, B. Hou, H. Yu, P. Vanýsek, M. Meron, B. Lin, I. Benjamin, and M. L. Schlossman, Proc. Natl. Acad. Sci. USA **109**, 20326 (2012).

[16] W. J. Huisman, J. F. Peters, M. J. Zwanenburg, S. A. de Vries, T. E. Derry, D. Abemathy, and J. F. van der Veen, Nature **390**, 379 (1997).

[17] L. Cheng, P. Fenter, K. L. Nagy, M. L. Schlegel, and N. C. Sturchio, Phys. Rev. Lett. **87**, 156103 (2001).

[18] P. Fenter and N. C. Sturchio, Prog. Surf. Sci. **77**, 171 (2004).

[19] M. Kinoshita, S. Iba, K. Kuwamoto, and M. Harada, J. Chem. Phys. 105, 7177

(1996).

[20] M. Kinoshita, J. Chem. Phys. **19**, 8969 (2003).

[21] R. Roth, M. Kinooshita, J. Chem. Phys. **125**, 084910 (2006).

[22] E. Kierlik and M. L. Rosinberg, Phys. Rev. A **44**, 5025 (1991).

[23] T. Sumi and H. Sekino, J. Phys. Soc. Jpn. **77**, 034605 (2008).

[24] I. K. Snook and W. van Megen, J. Chem. Soc. **77**, 181 (1981).

[25] A. Wallqvist and B. J. Berne, J. Phys. Chem. **99**, 2893 (1995).

[26] J. Gao, W. D. Luedtke, and U. Landman, J. Phys. Chem. B **101**, 4013 (1997).

[27] K. G. Ayappa and R. K. Mishra, J. Phys. Chem. B **111**, 14299 (2007).

[28] H. Matsubara, F. Pichierri, and K. Kurihara, J. Chem. Phys. **134** (2011) 044536.

[29] K. Kimura, S. Ido, N. Oyabu, K. Kobayashi, Y. Hirata, T. Imai, and H. Yamada, J. Chem. Phys. **132**, 194705 (2010).

[30] M. Watkins and B. Reischl, J. Chem. Phys. **138**, 154703 (2013).

[31] K. Amano, K. Suzuki, T. Fukuma, O. Takahashi, and H. Onishi, J. Chem. Phys. **139**, 224710 (2013).

[32] K. Amano and O. Takahashi, Physica A **425**, 79 (2015).

[33] K. Amano and E. Tanaka, arXiv: 1408.2730 (2014).

[34] J. G. Kirkwood, J. Chem. Phys. **10**, 394 (1942).

[35] Y. Karino, R. Akiyama, and M .Kinoshita, J. Phys. Soc. Jpn. **78**, 044801 (2009).

[36] Y. Kubota and R. Akiyama, J. Phys. Soc. Jpn. **81**, SA017 (2012).

[37] J. P. Hansen and L. R. McDonald, *Theory of Simple Liquids* (Academic Press, London, 1986).

[38] E. Lomba, Molc. Phys. **68**, 87 (1989).

[39] F. Taherian, V. Marcon, and N. F. A. van der Vergt, Langmuir **29**, 1457 (2013).

[40] P. Richetti and P. Kékicheff, Phys. Rev. Lett. **68**, 1951 (1992).

[41] J. C. Crocker, J. A. Matteo, A. D. Dinsmore, and A. G. Yodh, Phys. Rev. Lett. **82**, 4352 (1999).

[42] B. V. Derjaguin and I. I. Abrikosova, Nature **265** (1977) 520.

[43] J. N. Israelachvili, *Intermolecular and Surface Forces* (Academic Press, New York, 1992).

[44] K. Amano, K. Hashimoto, and R. Sawwazumi, arXiv:1505.04263 (2015).

[45] K. Amano, arXiv:1505.04360 (2015).

FIGURE CAPTIONS

Fig. 1. Schematic view of the system.

Fig. 2. Structures of the confined liquid. Blue solid, green dashed, red dotted curves are the results of 3D-OZ-HNC, RW theory, and SPRW theory, respectively. Values written in the tetragons represent s / d_S. The value $g_{tot} = \rho / \rho_0 = 1$ is located at the

horizontal dashed line for each case.

Fig. 3. Assessment of the deviation from the benchmark structure by means of RMSD. Green squares and red circles represent RMSD values of RW and SPRW theories, respectively.
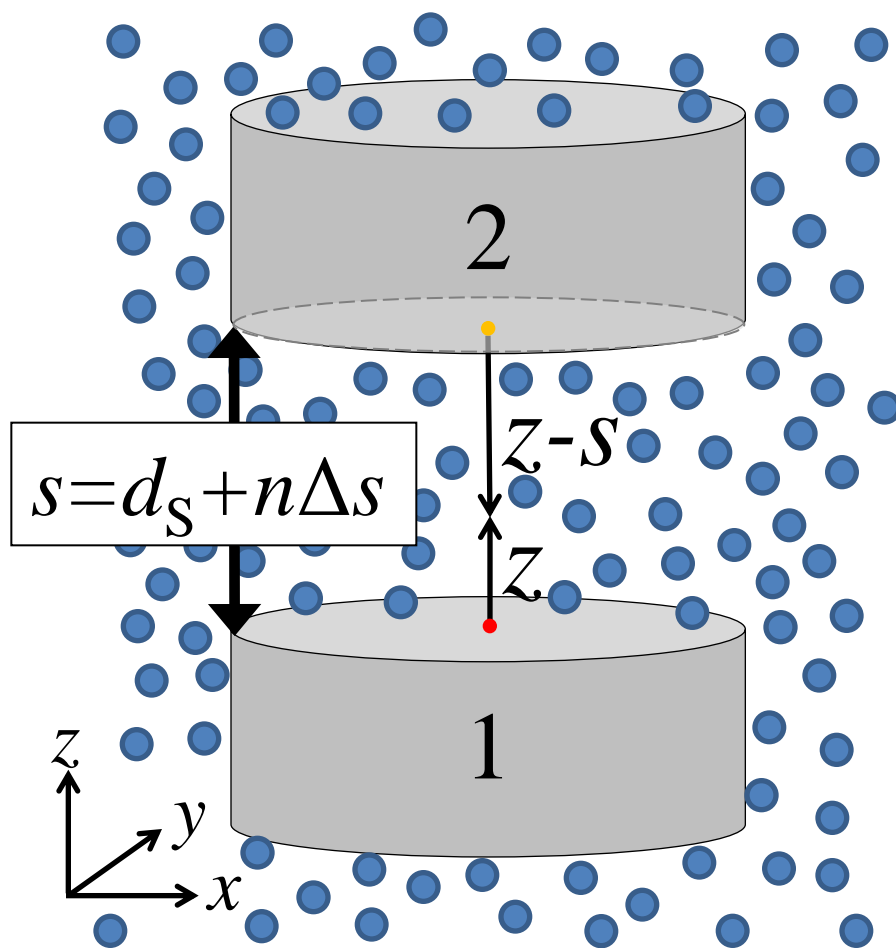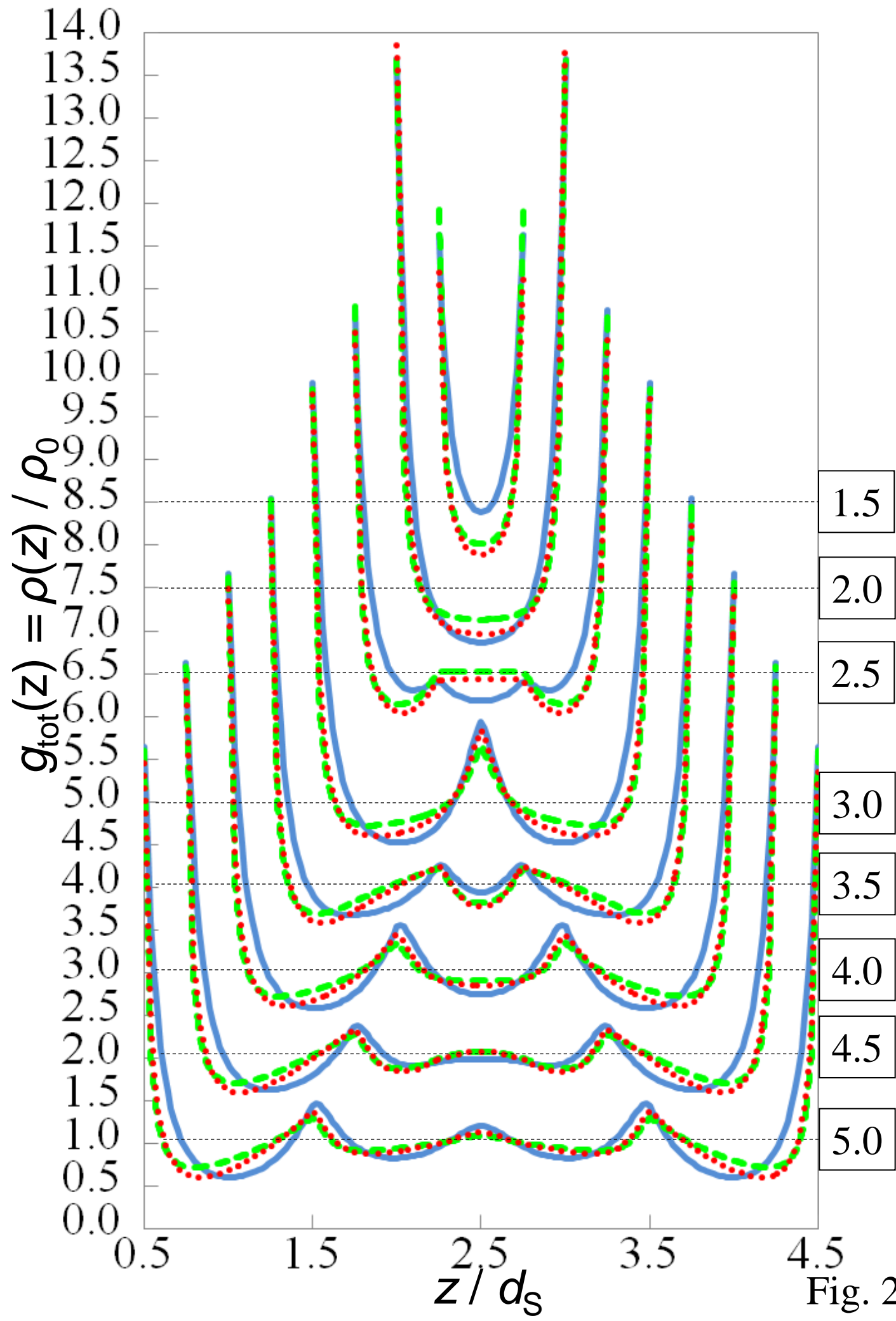
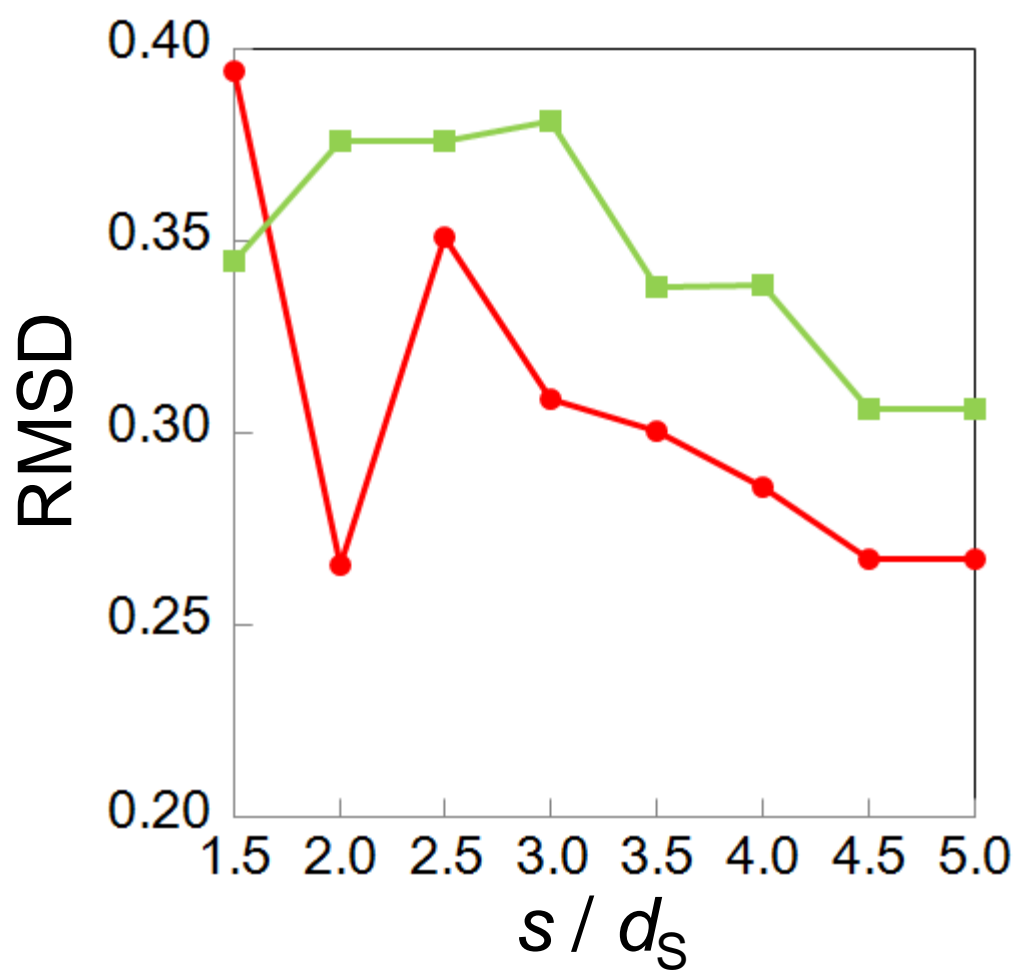$s=d_\mathrm{S}+n\Delta s$

Fig. 1

Fig. 2

Fig. 3